STIS Near-IR Fringing: Basics and Use of Contemporaneous Flats for Extended Sources

J. R. Walsh, S. A. Baum, E. M. Malamuth and P. Goudfrooij

ABSTRACT

A brief introduction to fringing in CCD chips is presented leading to a qualitative and quantitative discussion of the effect of fringes on STIS G750L and G750M spectra. G750L and G750M spectra of Jupiter's moon Io have been analyzed to study the efficacy of flat fielding of extended objects with tungsten flat field exposures taken together with the science data (i.e., contemporaneous flat). Spectra of Io taken at different positions along the slit and reduced with pre-flight pipeline flats and contemporaneous flats were compared assuming that only the flat field, and not the spectrum of Io, changed as the target was centered at different positions along the slit. For G750L, contemporaneous flat fields are essential if a signal-to-noise above 10 is required in the region of strong fringing—7000 to 10000Å. The residuals of the G750L fringes can be reduced below the 1% level by division by a well-exposed contemporaneous tungsten flat field. For G750M some advantage is displayed in the use of contemporaneous over pre-flight flats; however, the results are not conclusive since Io was drifting out of the slit during the course of the observations and the signal-to-noise on the spectra is less than 100. Further observations will be needed to better determine the signal-to-noise regime where contemperaneous flat fields are needed with G750M. In the interim, it is suggested that all observers using G750M longward of 7000 Å obtain contemperaneous flats with their science data. See STIS ISR 97-15 for information regarding insertion of such flats in Phase 2.

1. Introduction: Fringing on the STIS CCD

Fringing in CCDs results from multiple reflections between two surfaces where the distance between the surfaces (d) is a small integer (m) multiple of the wavelength of the incident monochromatic light. The small differences in path length gives rise to a series of bright and dark fringes. If the surfaces are parallel the fringe pattern is circular; if the seperation between the surfaces is a wedge, then the fringes can be nearly straight. In the case

of a CCD the front and back surfaces of the chip are never exactly planar or parallel and so the pattern of interference fringes may be rather irregular. The STIS CCD is a thin device and fringes are only important at the longer wavelengths. Since the CCD is primarily used for spectroscopy, the wavelength varies as a function of position along the dispersion direction, so the fringe pattern is some convolution of the contours of constant distance (*d*) between the front and back surfaces and the wavelength incident at that particular region of the CCD. For medium resolution data the wavelength changes slowly with position (~0.5 Å/pixel), so the shape of the CCD chip dominates the fringe behaviour; for low resolution data the wavelength changes much more rapidly (~5 Å/pixel), so the changing wavelength dominates. For STIS, since changes in MSM position (through non-repeatability, internal drifts, and changing MSM offsets) shift the resulting fringe pattern, the fringes will not be stationary with time and no one set of flat fields will suffice.

Since the low (G750L) and medium (G750M) resolution fringing have different physical causes, they are considered separately.

G750L fringing

The primary cause of the fringing is that λ varies strongly with *x* position on the detector, i.e., the changes in the surface separation as a function of position are small compared to the wavelength change from pixel to pixel. Since the dispersion direction only has a small tilt with respect to the x-axis of the detector, the contours of constant $d = m \lambda$ are therefore almost vertical (parallel to the slit), and so are the fringes. Figure 1 is a G750L image taken with the 52 x 0.1 slit at a central wavelength of 7751 Å. The large variation in the lamp brightness across the spectral range has been removed by fitting a spline curve through the data at the center of the image and dividing the result into each row. The slight tilt of the fringes is due to the fact that the surfaces of the chip are not exactly parallel. The fringe amplitude decreases toward the blue (left) side of this image. Table 1 provides the peak-to-peak and rms amplitudes of the fringes as a function of wavelength. Below 7000 Å the amplitude of the fringes is of the order or less than the counting statistics and so is not listed.

Tests on STIS ground-based data have shown that if a library of "fringe flats" is available then a fringe flat can be shifted by the proper amount to reduce the fringe amplitude of a given observation from about 25% to about 5% (peak-to-peak) provided that the wavelength settings of fringe flat and observation are within about 3 pixels. In order to improve the fringe removal a substantial library of fringe flats at one pixel shift intervals is required or else a fringe flat should be taken at the same time as the data.

G750M fringing

Figure 2 shows a pre-flight G750M image taken with the 52 X 0.1 slit with a central wavelength of 8561Å. In this case the wavelength changes from pixel to pixel are rela-

Figure 1: Ground fringe flat (continuum lamp exposure with the large scale trend removed) for the STIS CCD and G750L grating. The central wavelength is 7751 Å and wavelength increases to the right.

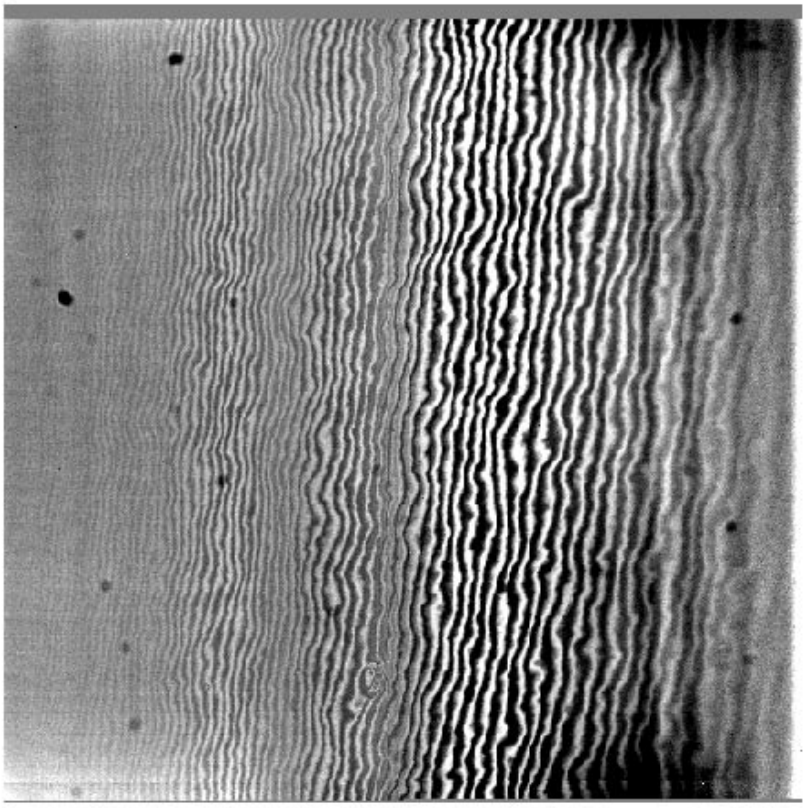

tively small, and so the fringe patter becomes dominated by the window separation changes. The fringes are also quite irregular, showing that the surfaces of the CCD are not exactly planar. Table 1 lists the fringe amplitudes for G750M for some central wavelengths.

For the G750M case, if a library of "fringe flats" at a set of given wavelength positions spaced about 3 pixels apart and of high S/N were to be built up, the user would be able to "flatten" the fringes to better than 1.5% by using the nearest "fringe flat" image (at most a shift of 1.5 pixels). A library at a finer spacing (about 1 to 2 pixels) would allow the user to "flatten" the fringes to better than 1%. Since it is difficult at best to command the MSM to a position within a couple of pixels a substantial library of fringe flats would have to be accumulated over a long period of time.

Figure 2: Ground fringe flat for the G750M grating. The central wavelength is 8561 Å and the range approximately 8270 to 8850 Å.

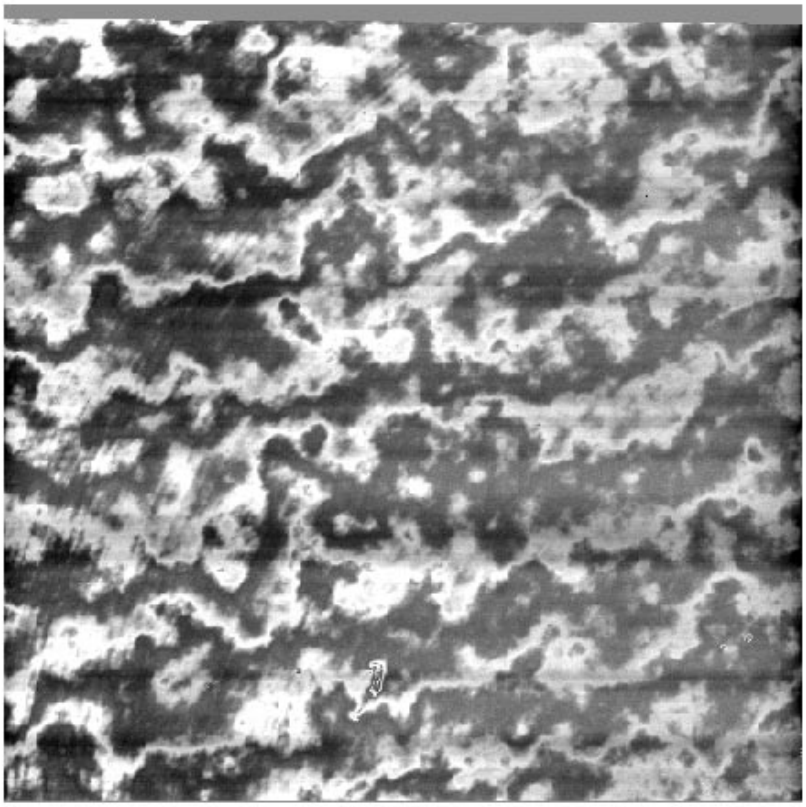

Table 1. Fringe amplitudes (%) for G750L and G750M

Wavelength	G750L		G750M	
	p-to-p	sigma	p-to-p	sigma
7250	3.18	2.13	4.62	1.52
7750	8.58	3.08	9.61	3.10
8250	6.76	2.80	10.53	3.26
8750	10.81	3.90	14.83	3.85
9250	23.42	7.90	27.16	9.00
9750	25.35	8.96	32.09	10.78
10250	17.30	5.89	18.23	6.04
10750	6.99	7.4	15.93	4.30

2. Fringe Removal on External Sources Using the Internal Lamps

A potential further complication in using fringe flat exposures to correct astronomical data is that the fringe flats are taken with an internal lamp while the data is from an external exposure. The light paths are slightly different and so also are the focal ratios of the beams. During the ground-based calibrations, a series of exposures were taken with the internal lamp and an external lamp in successive exposures without moving the MSM in order to evaluate how well an internal lamp could be used to correct an external exposure. Data with G750M, central wavelength 8561 Å showed very similar fringes from both the internal and external lamps; the results were consistent with no fringing being apparent above the photon counting statistics of the data (<1%).

The situation is somewhat different for the low resolution data where the difference in the wavelength is a much larger effect. Data for G750L, central wavelength 7751 Å, show residuals in the ratio of the external to the internal spectrum about 3% over the last 200 pixels (wavelengths above 9300Å) and somewhat lower from pixel 600 to pixel 800 (about 8200 to 9300 Å). The standard deviation over the entire 400 pixel range (about 8200-10250 Å) is just under 1%. Thus, it is not likely that fringes can be removed to much better than 2% using internal "fringe flats" for the 9000 to 10500 Å range.

The ground-based testing thus indicated that at least for G750L data, and possibly also for G750M data, fringe flats should be taken on-orbit if high signal-to-noise spectra are to be obtained in the 7000 to 10500 Å region with STIS. SMOV proposals were designed and implemented to test how well fringe removal could be performed for both point source and extended object data. The remainder of this ISR describes the testing as applied to extended object data and a subsequent ISR will describe the tests on point source data.

3. Observations

Cycle 7 calibration proposal 7605 consisted of 52x0.2" long slit spectra of Jupiter’s moon Io. The strategy was to obtain long slit data across the extended object (diameter of Io is 1.15") together with tungsten lamp exposures. The aim is to test the accuracy of flat fielding of extended objects using an identical slit to that of the science observations and taken during the course of the science data collection; this is referred to as a contemporaneous flat field. By moving the image of Io along the slit, the data are corrected by different regions of the flat field. Assuming that exactly the same region of Io is sampled (spectrum invariant), any differences in the spectra of Io must be attributable to uncertainties in the applied flat field. Experience has shown that adequate flat fielding can be achieved from pre-flight tungsten exposures, but only by shifting (in the dispersion direction) the flat field to the data. It is anticipated that contemporaneous flat fielding should do a superior job to shifted pre-flight flats; proposal 7605 was designed to test this supposition for extended objects. A separate proposal examined the applicability of contemporaneous flat fielding for point sources and will be reported in a follow-on ISR.

Observations were taken with the CCD and G750L grating (two pixel resolution 9.8Å and supported central wavelength 7751Å) and two tilts of the G750M grating (two-pixel resolution 1.12Å)—8561 and 10363Å. Table 2 lists details of the observations. Following the target acquisition using F28X50LP Longpass filter and a short direct image (0.1s, which was however saturated), observations were made at four pointings: centered on Io, and displaced +0.1,+ 0.5 and +2.0" in Y along the slit (set by POSTARGs) for each of the G750L and two G750M grating settings. The acquisition was not repeated before each sequence of spectral observations of Io. All exposures were taken with the 52x0.2" aperture. Preceeding and following each set of spectral observations of Io, a tungsten lamp exposure was made with the same slit.

Table 2. Observational Details

Target	Grating	Date	UT (TIME-OBS)	Dataset Name	Exp Time (s)	Mean Count (ADU)
Tungsten	G750L, 7751	1997-Jun-16	22:35:29	o42603020	15	1284.
Io			22:39:23	o42603030	24	2985.
Io +0.1"			22:44:20	o42603040	24	3044.
Io +0.5"			22:46:51	o42603050	24	3050.
Io +2.0"			22:49:23	o42603060	24	3055.
Tungsten			22:51:55	o42603070	15	1283.
Tungsten	G750M,8561		23:00:19	o42603080	75	1800.
Io		1997-Jun-17	00:01:42	o42603090	36	81.8
Io +0.1"			00:04:25	o426030a0	36	55.5
Io +0.5"			00:10:34	o426030b0	36	45.1
Io +2.0"			00:13:18	o426030c0	36	40.4
Tungsten			00:16:02	o426030d0	75	1793.
Tungsten	G750M,10363		00:22:57	o426030e0	75	560.
Io			01:44:09	o426030f0	108	3.6
Io +0.1"			01:48:04	o426030g0	108	3.7
Io +0.5"			01:54:05	o426040h0	108	3.7
Io +2.0"			01:58:01	o426030i0	108	3.9
Tungsten			02:01:57	o426030j0	75	554.

All the observations of Io and were made with no binning, in GAIN 4 and each was CR-SPLIT 2. For the tungsten lamp exposures, the set-up was identical except that no CR-SPLIT exposures were taken. It should be noted that these flat field exposures were made

with one bulb only on the lamp; the recommendations for GO added contemporaneous flats in ISR STIS 97-15 refer to two bulbs being on.

The last column of Table 2 lists the mean counts in the spectra; for the flat fields the mean refers to the whole chip (excluding the 20 first and last rows and columns) while for the Io spectra it covers only 28 columns centered on Io and the spectral extent excluding the first and last 20 channels. The final set of data of Io with G750M at 10363Å central wavelength has very low signal—only a few counts are visible in the Io spectrum. Subsequent to the observations it was found that the Io ephemeris had not been correctly uplinked and the moon was drifting out of the slit during the course of the observations. Therefore this set of observations, and the accompanying flats, were not analyzed. During the course of the second set of observations (G750M, 8561Å center) the counts in the spectrum were dropping from the first to the last dataset (difference of a factor 2), adding to the uncertainty in the analysis.

4. Data Analysis

Pipeline Reduction

The two sets of valid observations (G750L and G750M, 8561Å center) were analyzed identically. The data were recalibrated using CALSTIS with three different flat fields and the latest dark file (`h6h1352ro_drk.fits`—actually only valid for observations to 6 June, but the most recent available). The flat fields were as follows: 1) the pipeline flat-field, which is a pre-launch one provided by the Instrument Definition Team (B.S. Hill/ B.J. Hill Prelaunch flats—October 1996), `h230851ao_pfl.fits` for G750L and `h230851mo_pfl.fits` for G750M; 2) a dummy flat consisting of 1.0's; 3) a flat obtained by fitting and dividing a cubic spline though each line of the tungsten exposure using the iraf.noao.twodspec.longslit.response routine. This last will be referred to as the contemporaneous flat.

The pre-launch flat field used may not have been optimal in the sense that one with a more similar fringe-pixel mapping could have been chosen from the archive. Also some improvement in the derived data which was flat fielded by the pre-flight flat may have been possible by applying a shift (in one or both axes) to the flat, in order to better match the fringe pattern for Io; this was not attempted. No correction for scattered light along the slit length was made (Plait & Bohlin, 1997) for the tungsten lamp exposures, as any correction will be dependent on the spatial structure of the source.

To correct the contemporaneous flat, the following procedure was employed. The exposures of the tungsten before and after each sequence of observations on Io were compared and found to be similar both in level and features. They were averaged, with cosmic ray rejection (using noao.imred.ccdred.combine—ocreject could also be used) and the flat fields generated by the noao.twodspec.longslit.response task. For the G750L tungsten

exposure a cubic spline (SPLINE3) and ORDER 45 (number of spline pieces) was found to be adequate to fit the larger scale trends in the spectrum; for the G750M data a lower number of cubic spline sections (15) was sufficient as the spectrum is much flatter. Figure 3 shows cuts in the dispersion direction for G750L ground and in-flight flat fields, and Figure 4 the same for the G750M 8561Å data. More details of the spline fitting will be included in the forthcoming ISR on point source fringe removal.

Figure 3: The average flat field in the dispersion direction (rows 511-513 averaged) for the pre-flight G750L flat field (lower) and the contemporaneous flat field (upper) are shown. The latter was produced from the tungsten lamp exposures taken together with the spectra on Io.

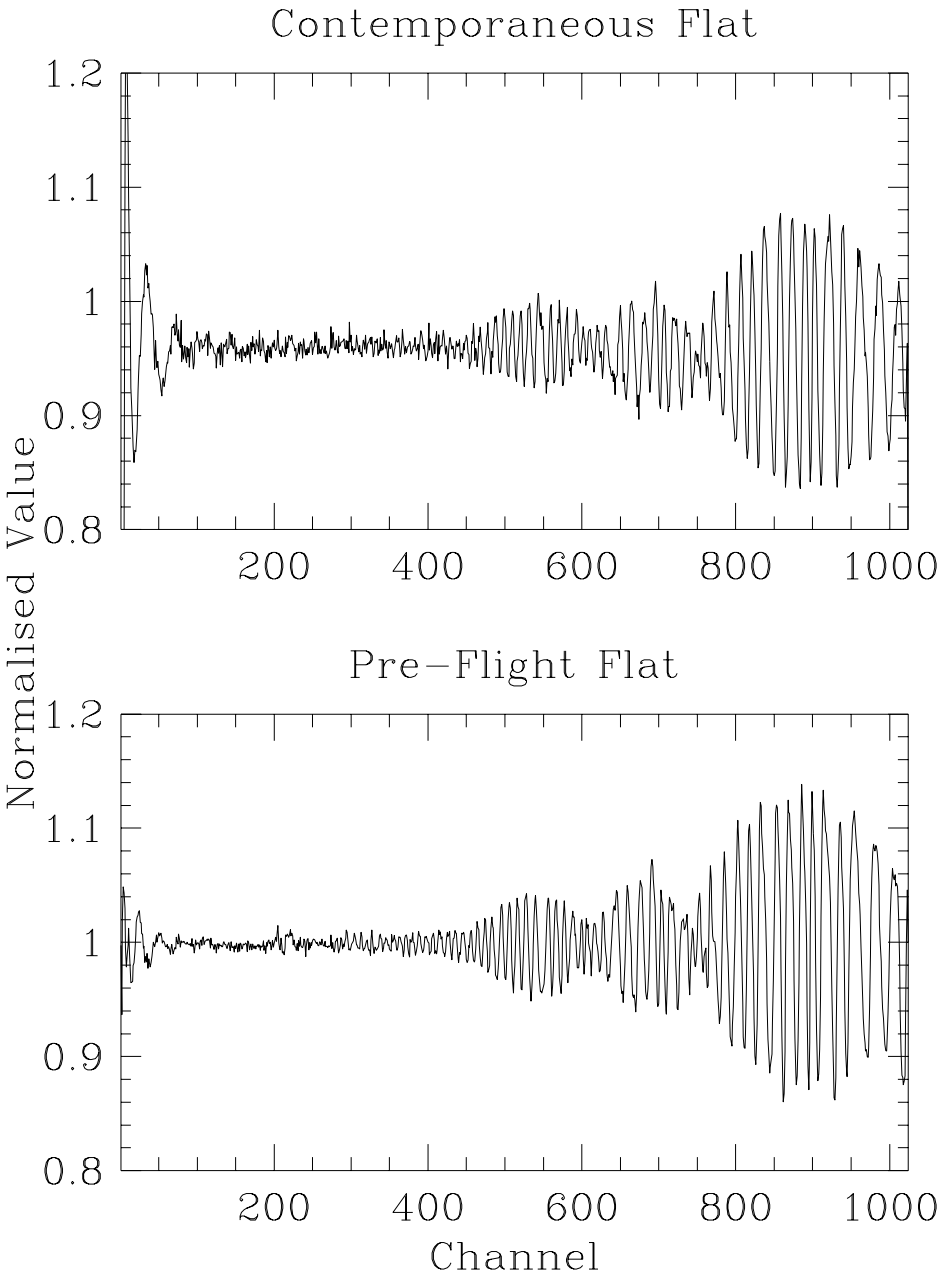

Figure 4: The mean flat field in the dispersion direction (rows 511-513 averaged) for the pre-flight G750M, central wavelength 8561Å, flat field (lower) and the contemporaneous flat field (upper), taken together with the spectra of Io, are illustrated.

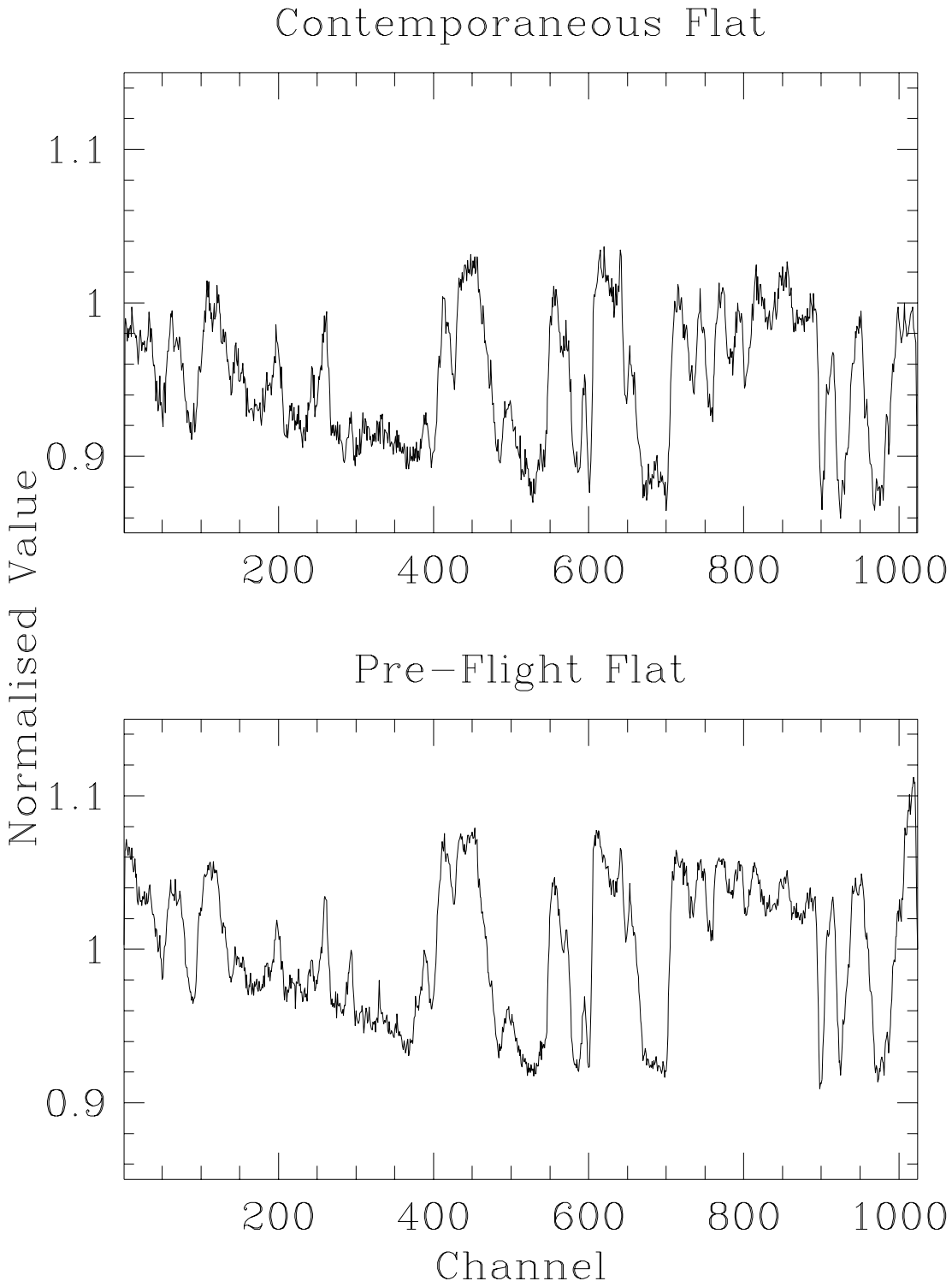

All the data were then pipeline calibrated with the PFLTFILE switch set to the appropriate flat field.

Fringe analysis

In order to consider the same spectrum for each set of four exposures with Io shifted along the slit, the spectrum was averaged over the same slit length at each position. Figure 5 shows the profile along the slit formed by summing most of the spectrum of Io for the G750L spectrum. An extent of 28 pixels (1.40") was taken as encompassing >97% of all the flux.

Figure 5: The profile of Io along the slit is shown. This spatial profile was formed by coadding most of the spectrum of Io from the G750L spectrum.

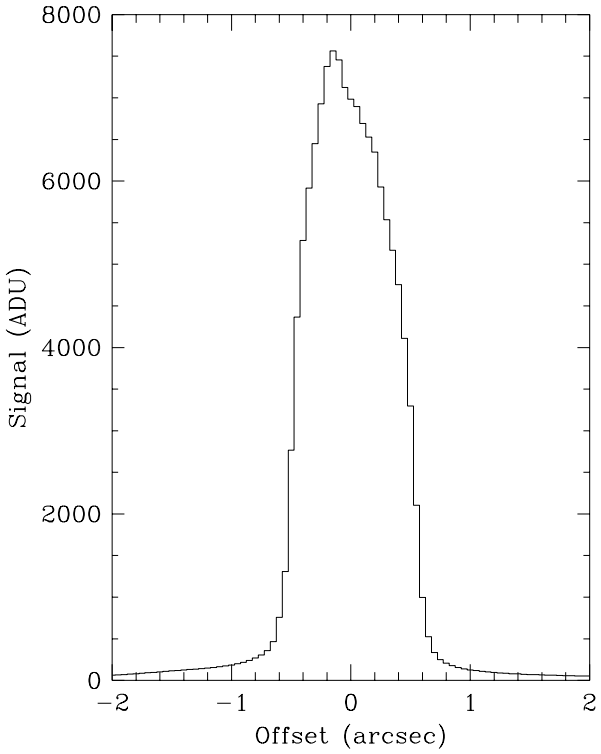

G750L

Figure 6 shows the four spectra produced with the contemporaneous flat field; there is some dispersion in the mean value—the slit position centered on Io showing a lower flux while the three spectra at offset positions show a higher but consistent flux. The difference between the center position and the mean of the other three resembles but is not identical to the average spectrum (it is redder) so may represent a real spectral difference rather than simply a region with higher albedo being centered in the slit (suggesting that the first slit positions did not cover an identical region of the surface to the other three). Figure 7a

shows the mean spectrum and the root mean square on the mean for the last three spectra (i.e., datasets o42603040, o42603050 and o42603060) for the pre-flight flat, and Figure 7b for the contemporaneous flat fielded data. The improvement in flat fielding resulting from use of the contemporaneous flat is marked. In order to quantify this improvement the ratio of the rms on the mean to the mean, expressed as a percent is shown in Figures 8a and 8b for the pre-flight and contemporaneous flat-fielded data respectively, again for the three last datasets only. Similar results are found if all four datasets are averaged, but the ratio of rms/mean shows a substantial (>1%) offset on account of the differing spectra.

Figure 6: The summed spectrum over Io (28 channels = 1.4 arcsec) for the four G750L exposures is shown. The first exposure (o42603030) is the lowest.

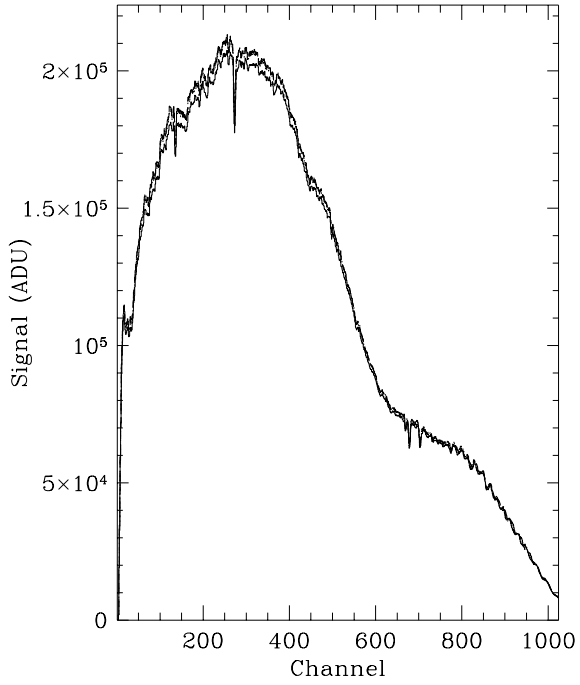

In order to derive a figure of merit for the improvement in flat fielding between the pre-flight and contemporaneous flats, the rms on the ratio (rms/mean) between the Io spectra could be used over the region of substantial fringing—taken as channels 500 to 850 (wavelength ~7630 to 9340Å). The longer wavelengths were not included since the signal from Io is low so the ratio is substantially affected by noise. Table 3 lists rms on the ratio (rms/mean) (in %) on the set of all four G750L Io spectra and for the three offset spectra (which had a consistent count) separately. The ratio of the rms's suggests a suppression of the fringing by a factor about 8 for contemporaneous over pre-flight flat fielded data. An alternative approach was to fit the large scale trends in the ratio (rms/mean) (Figures 8a and b), and compute the mean absolute deviation from this fit over the region of channels 500 to 850. This should be a better indicator of the correction at small spatial scales. The mean

absolute deviations are also listed in Table 3. The values for the four spectra averaged must be considered more uncertain on account of the differing spectrum of the central position. An improvement in flat fielding accuracy of a factor of about 8 is indicated from this Table.

Figure 7: a) The mean G750L spectrum of Io (bold curve) and the rms on the mean (dotted curve) from the three spectra at offsets +0.1, +0.5 and +2.0'' along the slit are shown. The spectra were reduced with the pre-flight flat field. The approximate wavelength scale (derived from the header) is also shown. b) As Figure 7a but for the spectra reduced with the contemporaneous flat field.

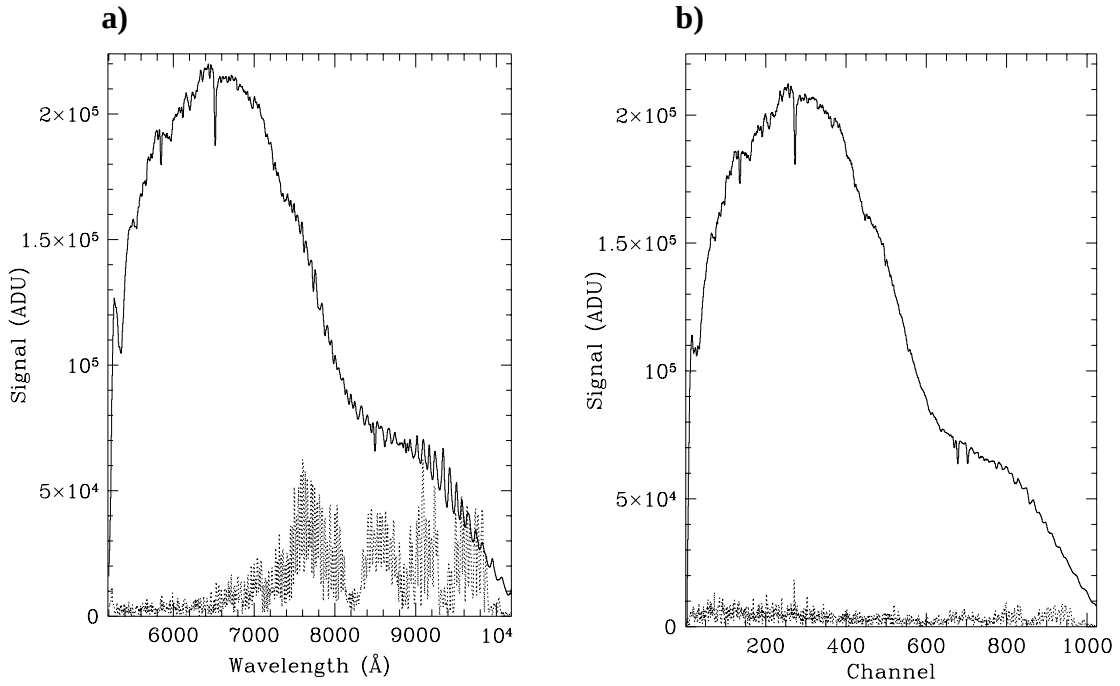

Table 3. Figures of Merit for Flat Fielding: Contemporaneous v. Pre-flight

	Pre-flight rms (%)	**Contemp. rms (%)**	**Merit**	**Pre-flight Mean dev. (%)**	**Contemp. Mean Dev. (%)**	**Merit**
G750L						
All 4 spectra	1.48	0.18	8.2	2.59	0.23	11.2
3 offset spectra	2.88	0.39	7.4	2.83	0.34	8.3
G750M 8561 Å	1.20	0.96				

Figure 8: a) The ratio of the rms on the mean of the three offset spectra (last three datasets) to the mean, expressed as a percent, for the G750L spectrum of Io. The spectra were reduced with the pipeline (pre-flight) flat field. b) As Figure 8a but for the spectra reduced with the contemporaneous flat field.

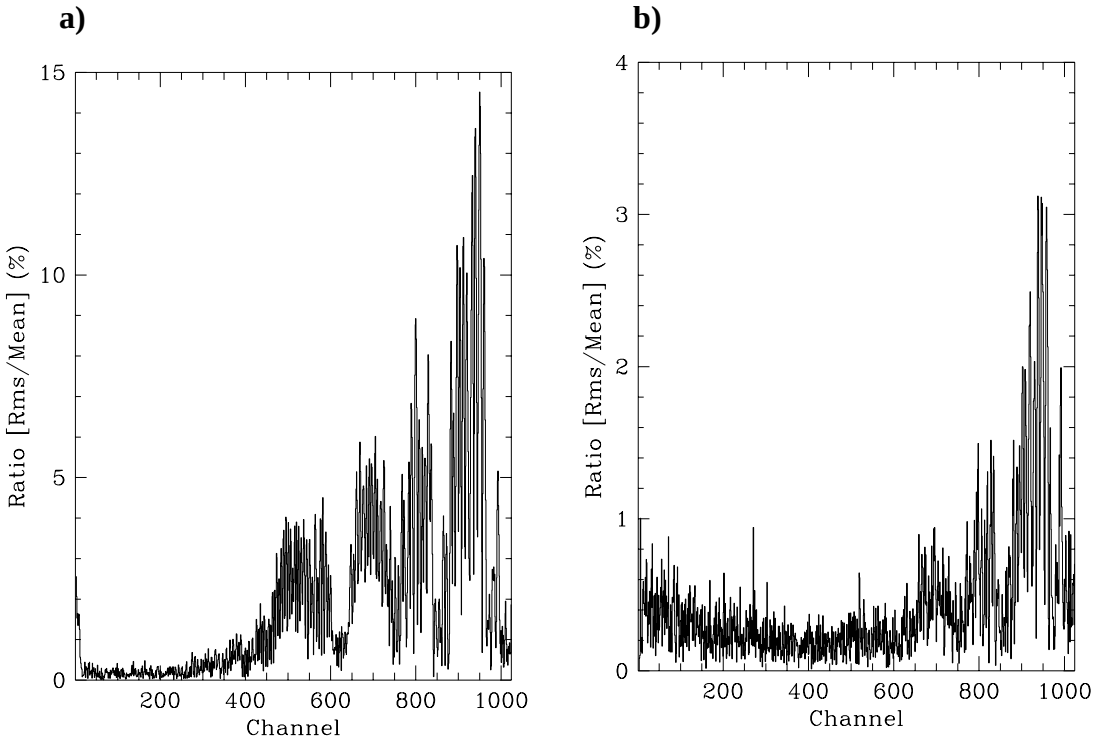

As a check that too much smoothing was not being introduced by averaging over the whole spectrum of Io (28 channels along the slit), extractions of the flat fielded spectra over half the extent of Io were compared. Ten channels on both sides of the peak were summed into spectra which were then ratioed. There is a slope term between the ratio for the two half spectra, similar to the difference between the centered and the three offset spectra. After removing this slope by fitting a low order polynomial, the rms on the ratio was measured. The ratio of the rms on the pipeline flat calibrated spectrum (5.4%) to that from the data which had been treated with the contemporaneous flat (0.9%) was 6.2, similar to the values found for the offset spectra. The slightly lower value for the figure of merit of contemporaneous over pipeline flat fielded data is attributable to the lower signal-to-noise of the data since only one dataset was checked in this manner.

The counts per pixel in the two 15s (single bulb) tungsten flat field spectra ensure that the statistical error of the flat field will vary from above 1.0% at low wavelengths (below 6500Å), peak at about 0.80% at around 9000Å and fall to 1.1% at 10000Å. (See Figure 12 for a plot of the count rate per pixel in a G750L 52x0.2’’ slit tungsten exposure). The pre-flight flat clearly has higher signal-to-noise than the contemporaneous flat, as is evident from Figure 3 where the pixel-to-pixel scatter is higher at the lower wavelengths in the

contemporaneous flat. G750L contemporaneous flats with a combined exposure time of 30s are capable of effectively removing the severe fringing in the 7200 to 9500Å region to the 1% level per pixel but the lower signal at shorter and longer wavelengths limits the flat field error to greater than 1% per pixel. The results of the comparison of integrated Io spectra taken at different positions along the slit demonstrate that the flat field correction is well behaved and the signal-to-noise on integrated spectra is not limited to the noise per pixel in the flat fields.

G750M

Figure 9 shows the four G750M, wavelength center 8561Å, Io spectra. The decrease in measured counts is obvious as Io drifted out of the slit. Figure 10a shows the mean and root mean square spectra for the slit offset four positions for the pre-flight flat, and in Figure 10b for the contemporaneous flat. The rms is of course dominated by the difference in level of the spectra. The ratio of the rms on the mean to the mean is illustrated in Figures 11a and b for the pre-flight and contemporaneous flat-fielded data respectively. Table 3 lists the rms on the ratio(rms/mean) in the G750M flat fielded data resulting from the pre-flight and contemporaneous flats. While an improvement is obvious it is not as dramatic as for the G750L case. Apart from the region of the absorption lines at 8500–8550Å, the improvement of contemporaneous over pre-flight flats is marginal. Given the signal-to-noise of the data (about 100) and possible positional variations as the slit swept across the moon, no strong conclusion can be drawn; better exposed spectra are required to test the flat fielding of G750M spectra to below the 2% level.

Figure 9: The summed spectrum over Io (28 channels = 1.4arcsec) for the four G750M exposures is shown. The strongest spectrum corresponds to the first exposure (o42603090) and the weakest to the last in the sequence (o426030c0).

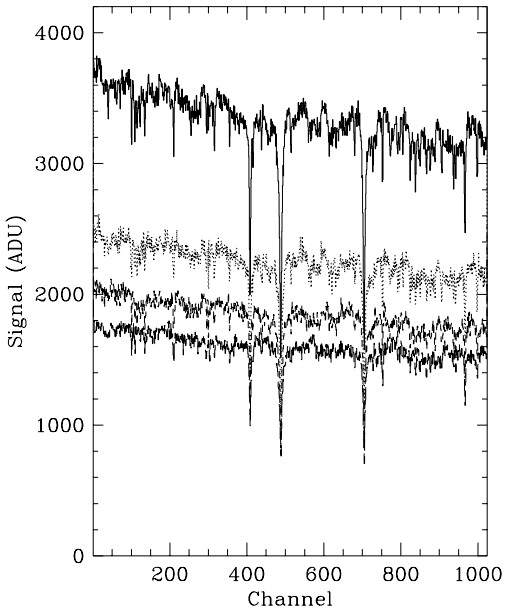

Figure 10: a) The mean G750M spectrum of Io (bold curve) and the rms on the mean (dotted curve) from the four exposures at different offsets along the slit are shown. The spectra were reduced with the pre-flight flat field. The approximate wavelength scale (derived from the header) is also shown. b) As Figure 10a but for the spectra reduced with the contemporaneous flat field.

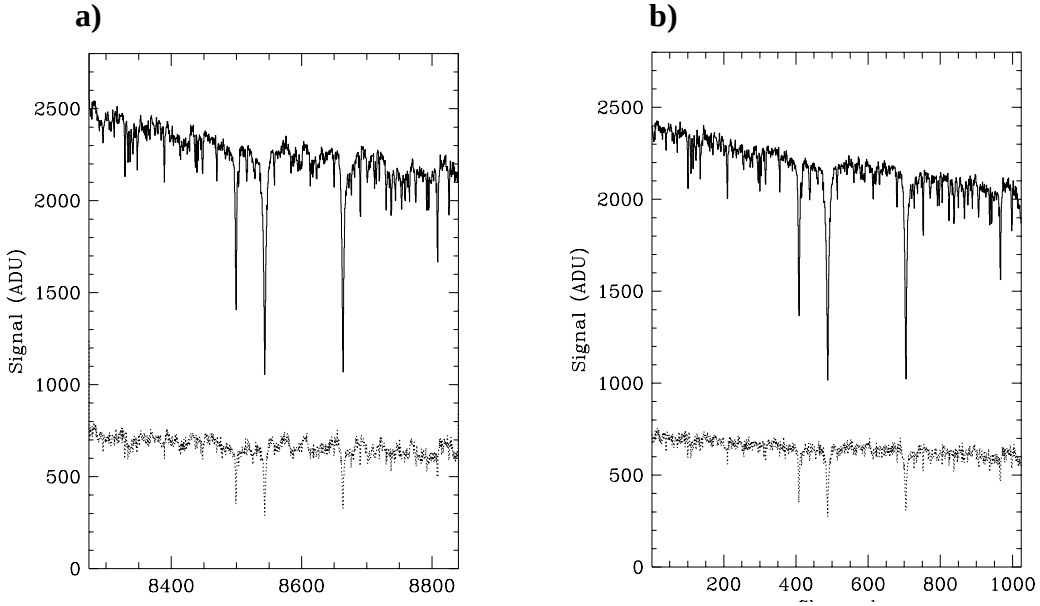

Figure 11: a) The ratio of the rms on the mean of the four offset spectra along the slit to the mean, expressed as a percent, for the G750M spectrum of Io. The spectra were reduced with the pre-flight flat field. b) As Figure 11a but for the spectra reduced with the contemporaneous flat field.

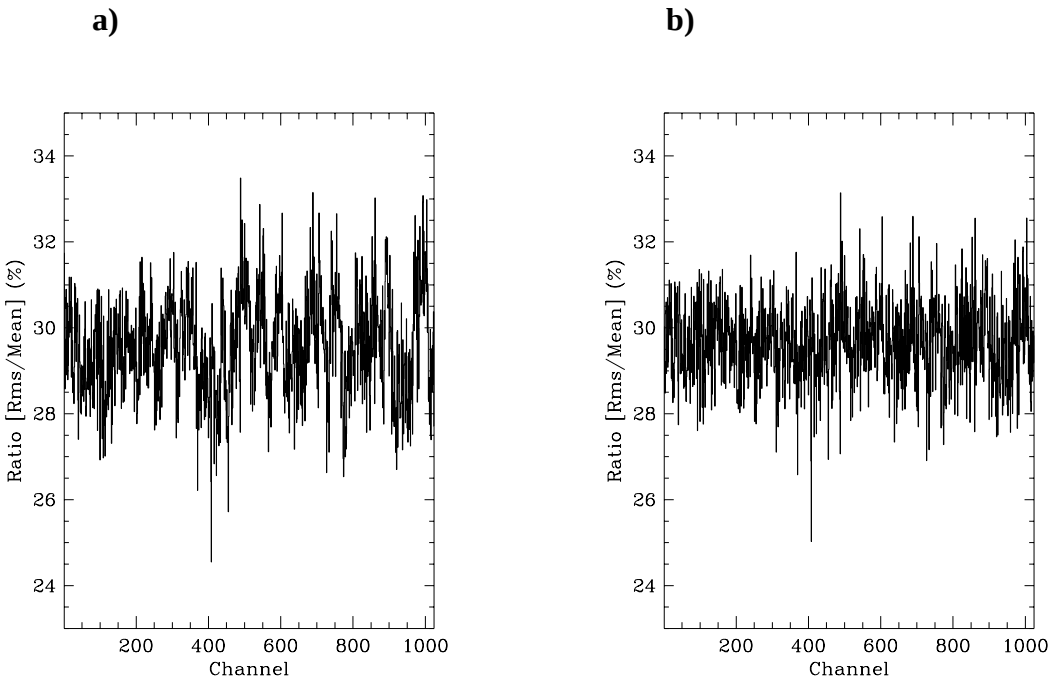

Figure 12: Count rate (ADU per pixel per second) for two 1-d cuts (channels 511-513 averaged) across the tungsten lamp image for the G750L grating (wavelength center 7751Å) taken from the mean of the two tungsten lamp exposures (see Table 2). The lower cut is in the wavelength direction and the upper one along the slit. The slit width was 0.2".

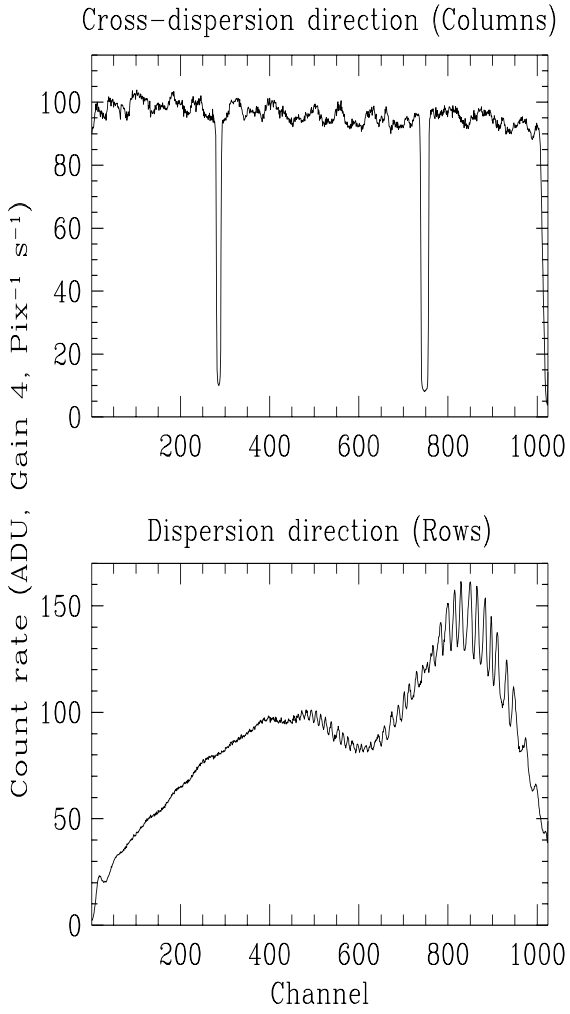

5. Conclusions and Recommendations

On the basis of the differences in the spectra of Io taken at four different positions of the target along the slit, the following recommendations can be made concerning contemporaneous flat fielding for extended sources:

1. The flat field amplitude for G750L approaches 15%, and for G750M, 8851Å tilt 7%.

2. For G750L, contemporaneous flat fielding is essential if exploitation of the data at wavelengths above 7500Å at signal-to-noise ratios exceeding 10 is required. Since there are no significant lifetime constraints, contemporaneous flats should be obtained routinely with all G750L observations.

3. With the current tungsten lamp, two single-bulb exposures of 15s each are sufficient to allow flat fielding to slightly better than 1% per pixel from 7000 to 9500Å and above 1.0% per pixel beyond 9500Å and less than 6500Å for G750L data with the 0.2” wide slit (based on statistical errors alone). Figure 12 shows the count rates (ADU per pixel per second) for two cuts in the dispersion and cross-dispersion directions (channels 511–513 averaged) for the G750L tungsten lamp exposure. At wavelengths shortward of 7000Å the low counts in two 15s tungsten lamp exposures limit the flat fielding accuracy to above 1.0%. However, the fringing is not available and the pipeline plot can be used. Note however that these exposures were obtained with only one lamp switched on; GO added fringe flats are obtained with two lamps.

4. For G750M at 8561 Å, a pair of single-bulb tungsten exposures of at least 50s each are required for adequate flat fielding.

5. For G750M, flat field residuals of 1.2% (rms) (3% peak amplitude) remain after flat fielding by pre-flight flats. Using a contemporaneous flat, the rms drops to 0.95% and has fewer large scale features.

6. The case for contemporaneous flat fielding of G750M data appears to be marginal if a signal-to-noise ratio of less than about 50:1 is required. Contemporaneous flat fields may be necessary if higher signal-to-noise is needed but deeper spectra are required to establish this. In the interim it is recommended that GOs always obtain contemporaneous flats for G750M data at wavelengths beyond 7000 Å.

6. References

Baum, S., Ferguson, H., Walsh, J. R., Goudfrooij, P., Downes, R., 1997. “GO Added Near-IR Fringe Flats” STIS ISR 97-15 Plait, P., Bohlin, R., 1997. In *1997 HST Calibration Workshop*, eds. Casertano, S. et al., STScI.